Colloids and Surfaces A 568 (2019) 36–42

Contents lists available at ScienceDirect

Colloids and Surfaces A

journal homepage: www.elsevier.com/locate/colsurfa

Hydrophobic agglomeration behaviors of clay minerals as affected by siloxane structure

Weiquan Zhan[a], Hao Yi[a,*], Shaoxian Song[a,b], Yunliang Zhao[a,b,*], Feng Rao[c]

[a] Hubei Key Laboratory of Mineral Resources Processing and Environment, Wuhan University of Technology, Luoshi Road 122, Wuhan, Hubei, 430070, China
[b] School of Resources and Environmental Engineering, Wuhan University of Technology, Luoshi Road 122, Wuhan, Hubei, 430070, China
[c] Instituto de Investigación en Metalurgia y Materiales, Universidad Michoacana de San Nicolás de Hidalgo, Ed. "U", Ciudad Universitaria, Morelia, Michoacán, 58030, Mexico

GRAPHICAL ABSTRACT

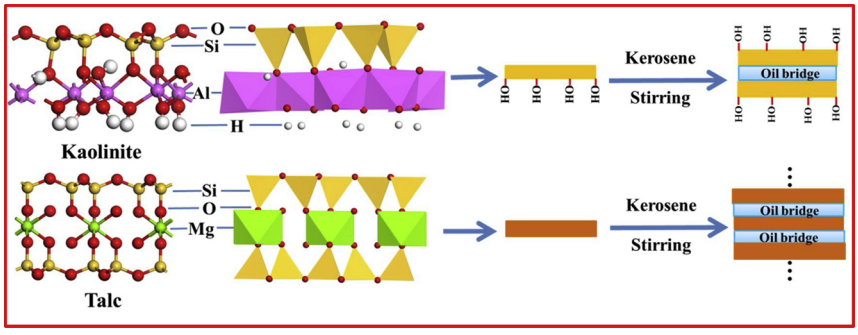

ARTICLE INFO

Keywords:
Siloxane structure
Hydrophobic agglomeration
Talc
Kaolinite

ABSTRACT

Due to the very hydrophobic characteristic, silica tetrahedron (siloxane) structure on clay minerals surfaces was believed to affect many surface property of clay minerals, such as surface wettability, dispersion and agglomeration property. In this work, kaolinite and talc, with different number of siloxane surfaces, were chosen for studying how the siloxane structure affected hydrophobic agglomeration behaviors in aqueous solution. In-situ turbidity measurement of flocs suspension in the settlement progress had been applied to characterize the agglomeration behaviors of clay minerals. Through molecular dynamics simulation (MDs) results, it was found that the hydroxyl surface of kaolinite was very hydrophilic, while the siloxane surface of kaolinite (on the Si-tetrahedral side) and talc (both basal surfaces) showed a strong hydrophobicity due to the highly symmetrical siloxane structure. As a result, the talc and kaolinite showed vast differences on hydrophobic agglomeration behaviors. Because of the much more exposed siloxane structures on talc surface, the hydrophobic agglomeration degrees are far stronger than that of kaolinite due to the both hydrophobic basal surfaces. Besides, the sizes of talc flocs are also far larger than that of kaolinite due to the formation of layer by layer floc structure. Therefore, the siloxane structure on clay minerals surface has a significant influence on the agglomeration behaviors, including the agglomeration degree and the size of resulted flocs. It is the first time that the hydrophobic agglomeration behaviors were correlated to the siloxane structure on clay mineral surfaces, which has profound guiding significance on the study of dispersion stability of colloidal clay minerals.

* Corresponding authors at: Hubei Key Laboratory of Mineral Resources Processing and Environment, Wuhan University of Technology, Luoshi Road 122, Wuhan, Hubei, 430070, China.
E-mail addresses: yihao287@whut.edu.cn (H. Yi), zyl286@whut.edu.cn (Y. Zhao).

https://doi.org/10.1016/j.colsurfa.2019.01.061
Received 20 November 2018; Received in revised form 29 January 2019; Accepted 29 January 2019
Available online 30 January 2019
0927-7757/

1. Introduction

Clay minerals are important non-metallic mineral, which has been widely used as adsorbents, catalysts and pharmaceuticals [1–3]. And the dispersion or aggregation behaviors of clay minerals played significant role in their applications. In the field of clay-polymer composite materials, the uniform dispersion of clay minerals enabled the composite much better performances [4,5]. As for the application of adsorbents, the dispersion of clay minerals provided much larger specific surface area for the adsorption of pollutants [6,7]. The agglomeration of clay minerals is also very important in industrial applications. In environmental fields, the aggregation of clay minerals after adsorption of pollutants was essential to separate the adsorbents [8,9]. In mineral processing, flocculation-flotation was a very commonly method to recover fine clay minerals [10]. As for the solid-liquid separation technique, the fast aggregation of fine clay minerals promoted the efficient recycling of water resource [11]. Compared with dispersion of clay minerals, the aggregation of clay minerals has much wider applications in actual industrial productions, which leads to the much more powerful attraction of researches in aggregation of clay minerals.

There were several commonly used methods to aggregate the fine particles in aqueous solutions, such as coagulation, polymer flocculation and hydrophobic agglomeration [12,13]. Due to the formation of large and compact flocs, the hydrophobic agglomeration had been applied more widely [14]. Hydrophobic agglomeration was a way to aggregate fine particles by the hydrophobic attraction between the particles [15]. Surfactants had been usually added in a number studies to show how the wettability of particles reduced for enhancing flocs size [16–19]. However, surfactant modified particle does not show very strong hydrophobicity, and the resulted hydrophobic agglomeration is not very strong [20–23]. Therefore, it was vital to seek a more efficient method for enhancing flocculation performance.

Generally, clay minerals are layered aluminosilicate minerals with silica tetrahedron sheet and alumina octahedral sheet stacked on each other. Silica tetrahedron, also called siloxane, is a nonpolar structure, the hydrophobic properties of which had been widely studied. Malandrini et al. [24] had concluded that the external oxygen atoms on the siloxane surface were relatively weak electron donors and showed very weak interactions with water molecules [25]. Tarasevish et al. [26] had also verified the very weak interaction between siloxane surfaces of talc and water molecules. Also, the nature of the siloxane surface in smectites was demonstrated to be hydrophobic by measuring the adsorption of aromatic hydrocarbons [27]. As for the hydroxyl surface in TO structural clay mineral, it was obviously to be of hydrophilicity. Šolc et al. [28] had researched both the contact angle of siloxane surface and hydroxyl surface in kaolinite through molecular dynamics simulation (MDs), it was found that the contact angle of octahedral surface was equal zero while the contact angle of the tetrahedral surface was about 105°. Yin et al. [29] had drawn similar conclusions that the siloxane surface of kaolinite showed hydrophobicity while alumina octahedral face displayed no hydrophobicity at all. As a result, the siloxane surface led to the hydrophobic character of clay minerals while hydrophilicity arose from the hydroxyl groups on clay mineral surface [30]. In other words, surface wettability of clay minerals was determined by the siloxane structure to a large extent. Considering that the contact angle of siloxane surface of clay minerals is often greater than 100°, which are larger than that induced by surfactants.

The siloxane structure on clay mineral had turned out to be of strong hydrophobicity. At the same time, wettability had a significant influence on the colloidal stability of clay minerals [10,31]. It was reported that larger contact angle of talc particles had stronger hydrophobic attraction, which leads to more powerful aggregation [32]. Duzyol et al. [33] had studied the correlation of agglomeration of dolomite with its wettability, it was found that the agglomeration of the particles required a lower wettability. Xuan et al. [34] had also proved higher agglomeration due to the decrease of its wettability. Hence, the very hydrophobic siloxane surface of some clay minerals may lead to much more powerful hydrophobic agglomeration performances.

Therefore, the TOT and TO structural clay minerals, distinguished by the exposed surfaces, were supposed to show distinct differences in hydrophobic agglomerations. However, to our best knowledge, no reports had correlated siloxane structure of clay minerals with hydrophobic agglomeration behaviors, despite that numerous researchers had investigated the hydrophobic agglomeration behaviors of clay minerals in aqueous suspensions [35–37]. Thus kaolinite consist of one siloxane surface and one hydroxyl surface as well as talc comprised of two siloxane surfaces were chosen for studying how the siloxane structure on the clay mineral surface affected hydrophobic agglomeration. Considering that the MDs can be used to study the interactions between liquid nanodroplets and mineral surfaces [38–44], wettability of both siloxane surface and hydroxyl surface were investigated through MDs. Besides, since most of traditional methods to measure particle size could not apply to the flocs which are easily to be destroyed when dried or filtered, thus in-situ turbidity measurement was applied for researching the hydrophobic agglomeration differences between talc and kaolinite fines in aqueous suspensions [45]. The objective of this work is to correlate the siloxane structure on clay mineral surfaces with the hydrophobic agglomeration behaviors, thus to provide profound guiding significance on the study of dispersion stability of colloidal clay minerals.

2. Experimental

2.1. Materials

The original talc sample was obtained from Aladdin Industrial Corporation and kaolinite mineral sample was used. D8 Advance X-ray diffract meter (Bruker, Germany) was used for analyzing the samples. The X-ray diffraction (XRD) pattern of talc and kaolinite had been displayed in Figs. 1 and 2, respectively, showing that talc and kaolinite particles were both of high purity.

The particle size distributions of the talc and kaolinite samples were estimated by a Malvern Mastersizer 2000 (Malvern, England). As illustrated in Fig. 3, talc particle size at the D_{50} and D_{90} (particle size at 50% and 90% cumulative undersize) were of 8.3 μm and 18.0 μm, respectively, and the D_{50} and D_{90} of kaolinite size were of 8.0 μm and 16.8 μm, respectively. The results indicated that talc and kaolinite particles were about the same size.

Ultrapure water with the electrical resistivity of 18.2 MΩ cm was produced by Millipore Super Q system (Millipore, America), thus to minimized the effects of impurities in water.

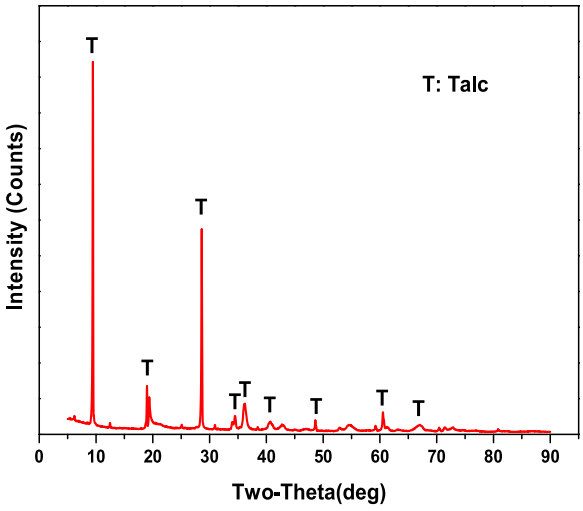

Fig. 1. XRD patterns of the talc sample.

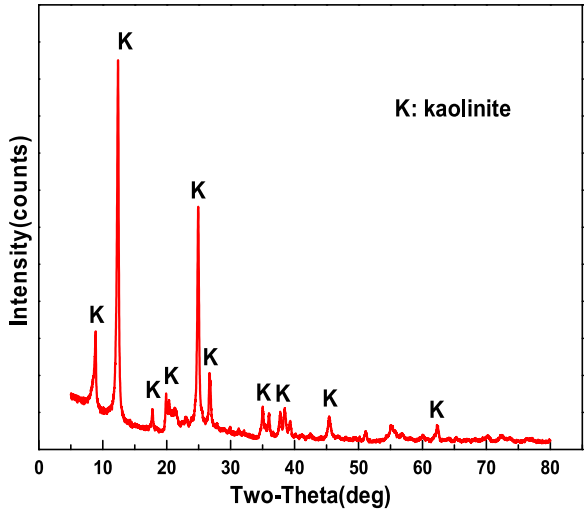

Fig. 2. XRD patterns of the kaolinite sample.

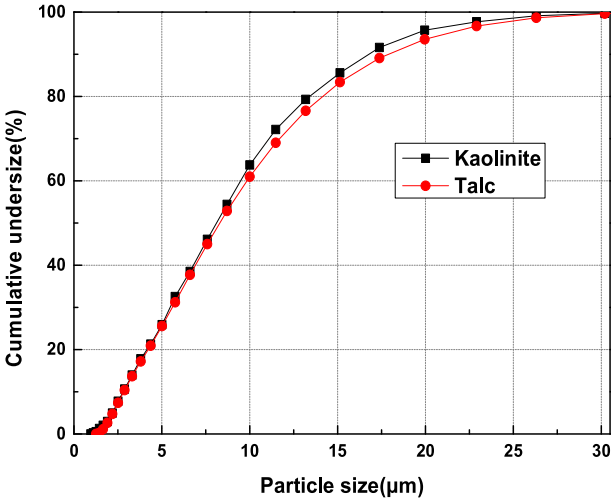

Fig. 3. Particle size distribution of the talc and kaolinite samples.

2.2. Hydrophobic agglomeration of talc and kaolinite

The hydrophobic aggregation experiments were carried out in a standard tank with four baffles and six blades described in previous literatures [3,32,45]. Likewise, clay minerals (talc, kaolinite) suspension with 0.3% solid concentration were prepared as described in previous works [32,45]. After that, the suspension was stirred in the aggregation tank, the kerosene was added simultaneously. Then the in-situ turbidity of the suspension was measured every 5 s in a Turb 555 IR nephelometer (WTW, Germany) in sedimentation progress. Finally, the computer connected to the nephelometer collected the data.

As described in previous works [32,45], the turbidity of flocs suspension as a function of time was aimed to fit a specific function, and the nonlinear fitting equation was shown below:

$$y = A_1 \times \exp\left(-\frac{x}{t_1}\right) + y_0 \quad (1)$$

It could be converted into a linear equation as follows:

$$\ln(y - y_0) = \ln A_0 - \frac{x}{t_1} \quad (2)$$

In which y denotes the turbidity of the clay mineral flocs suspension; x is the sedimentation time; and y_0, A_1 and t_1 represent corresponding constants.

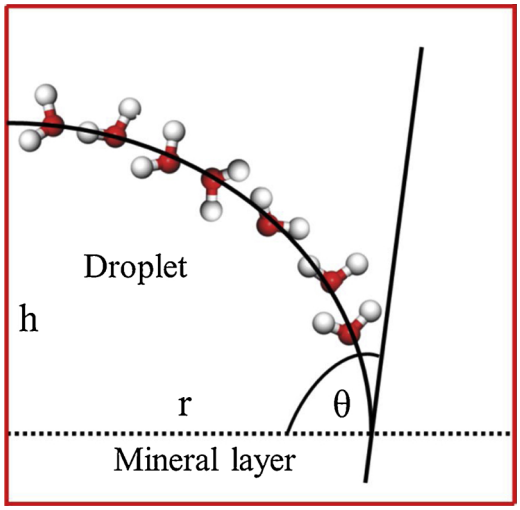

Fig. 4. Schematic of computation of water-gas boundary and contact angle θ, h is the height from the mineral layer, and r represents the base circle radius of water droplet.

The slope K of Eq. (2) assesses the average size of the flocs formed by clay mineral fines after being flocculated, which is defined as:

$$K = \frac{1}{t_1} \quad (3)$$

The agglomeration degree E evaluates the dispersion and agglomeration of clay mineral fines, which can be expressed as:

$$E = \frac{T_0 - T_E}{T_0} \times 100\% \quad (4)$$

In which T_0 and T_E represent the initial and ultimate turbidity of the flocs suspension, respectively.

2.3. MDs of wettability on kaolinite and talc surface

MDs in this work were carried out in Forcite module of Materials Studio 8.0. The water droplet was modeled by the 300 SPC/E water model. The atomic positions in the layer model of kaolinite were taken from the experimental neutron power diffraction experiment [46]. The space group of kaolinite was C1; unit cell parameters were as follows: a = 0.514899 nm, b = 0.893400 nm, c = 0.738400 nm, and α = 91.930°, β = 105.042°, γ = 89.791°. The initial configuration of talc was constructed using lattice parameters provided by American Mineralogist Crystal Structure Database [47]. The space group of talc was C2; and the fundamental cell parameters were listed below: a = 0.526 nm, b = 0.91 nm, c = 1.881 nm, and α = γ = 90°, β = 100°. The size of each cell was obtained through multiplication of experimental a, b, and c vectors. A model of isolated kaolinite layer possessing both (001) and (00−1) basal surfaces and a model of isolated talc layer possessing (001) basal surfaces were built. The droplet was positioned in the middle of the computational cell at a distance of ˜3 Å from the mineral surface to the bottom border of the droplet. The first dynamic model was represented by water droplet placed on the (001) hydroxyl surface of the kaolinite layer with a cell size of 4.1192 × 4.4670 × 9.4595 nm. The second dynamic model was constructed from the water droplet deposited on the (00−1) siloxane surface of the kaolinite layer with a cell size of 4.4670 × 4.1192 × 9.4595 nm. The third dynamic model was consisted of the water droplet placed on the (001) siloxane surface of the talc layer with a cell size of 4.2080 × 4.5500 × 11.1788 nm. In this simulation, apart from clay mineral and water droplet, a vacuum slab with a height of 5.0 nm was needed to put on the amorphous cell. Thus, the whole simulation cell under periodic boundary conditions had been built up.

The clay force field (CLAYFF) was used for describing the

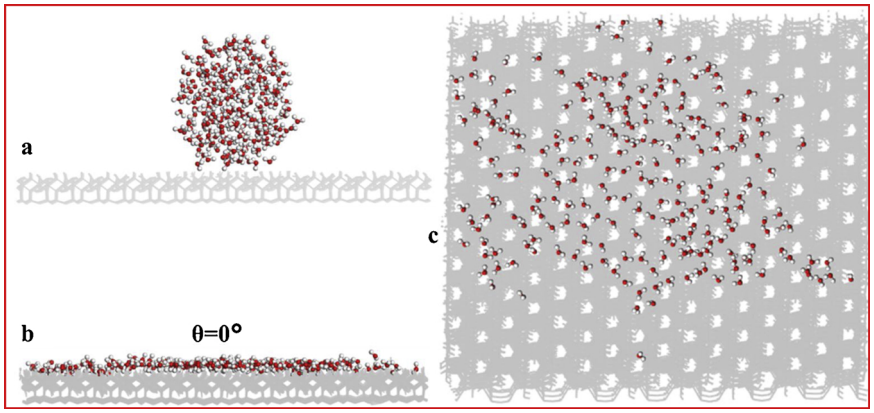

Fig. 5. Snapshots from MDs for water droplet placed on the (001) hydroxyl surface of kaolinite layer: initial geometry (a), front (b) and top (c) view after 200 ps.

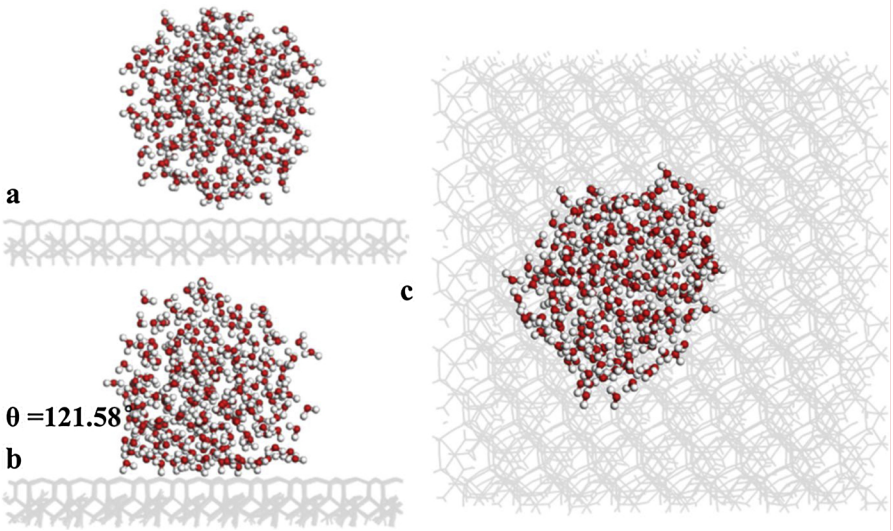

Fig. 6. Snapshots from MDs for water droplet placed on the (00 − 1) siloxane surface of kaolinite layer: initial geometry (a), front (b) and top (c) view after 200 ps.

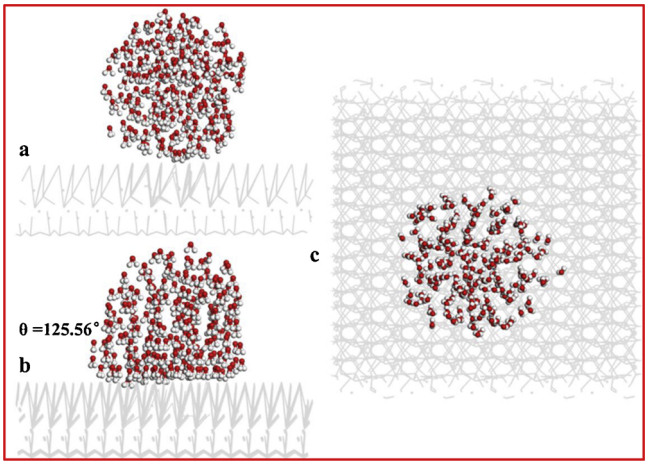

Fig. 7. Snapshots from MDs for water droplet placed on the (001) siloxane surface of the talc layer: initial geometry (a), front (b) and top (c) view after 200 ps.

interatomic potentials for the clay mineral surface and water droplet. In MDs, the geometry optimization task was first carried on the structure models. After that, the NVT ensemble (the particle number (N), volume (V), and temperature (T) were constant) was selected to equilibrate the structure of the systems. The simulation time was set as 200 ps to make the system get equilibrated. The time step and temperature were 0.2 fs and 298 K, respectively.

In simulations, a microscopic contact angle was computed from a fit of circle equation to contour of water droplet as shown in Fig. 4. By measuring the relevant length parameters, the equation which associated contact angle and the parameters was as follows:

$$\tan\left(\frac{\theta}{2}\right) = \frac{h}{r} \tag{5}$$

It can be transformed into another form:

$$\theta = 2\text{arc} \quad \tan\frac{h}{r} \tag{6}$$

Where θ is contact angle, h is the height from the mineral layer, and r represents the base circle radius of water droplet.

3. Results and discussion

3.1. Effect of siloxane structure on the surface wettability

Snapshots from MDs for wettability of hydroxyl surface of kaolinite, siloxane surface of kaolinite and siloxane surface of talc were represented in Figs. 5–7, respectively. The results showed that the water droplet was completely spread on the hydroxyl surface of kaolinite, which indicated the strong hydrophilicity of hydroxyl surface (contact angle = 0°). As for the siloxane surface of clay minerals, the water droplet only slightly spread on the basal surfaces, which suggested the

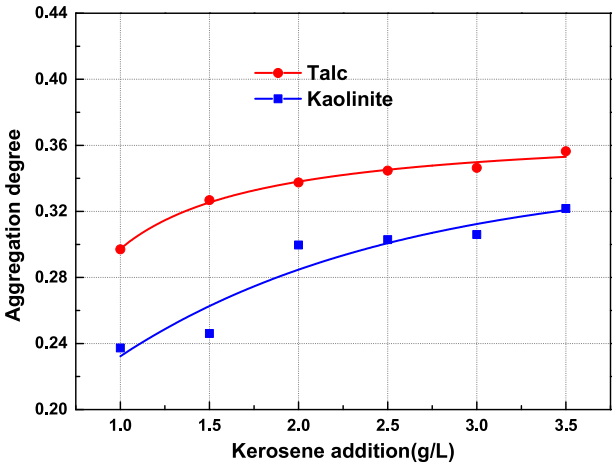

Fig. 8. Effect of kerosene addition on aggregation degree.

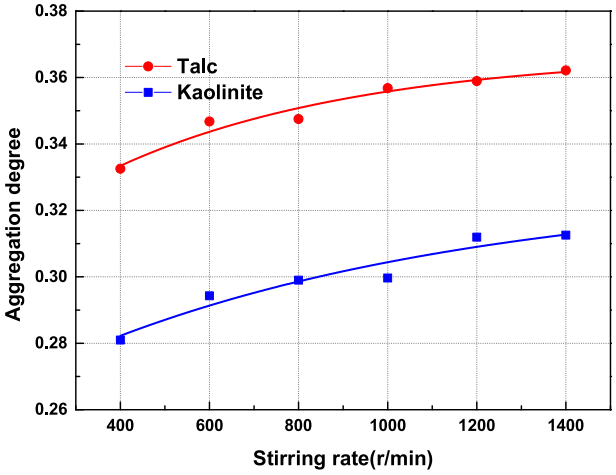

Fig. 9. Effect of stirring rate on aggregation degree.

strong hydrophobicity of siloxane surfaces. According to Eq. (6), the computed contact angle of siloxane surface of kaolinite and talc were 121.58° and 125.56°, respectively. This results were in good agreement with previous study [48], which also demonstrated the hydrophobicity of siloxane structure on clay mineral surfaces. Due to the existence of plenty of hydroxyl group, water molecules could form hydrogen bond with hydroxyl surfaces, which account for the strong hydrophilicity of the hydroxyl surfaces of kaolinite [49]. On the contrary, the interaction between water molecules and siloxane surface was weak due to the

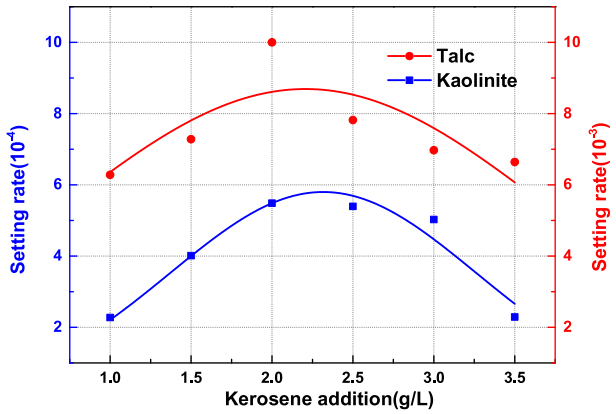

Fig. 10. Effect of kerosene addition on setting rate.

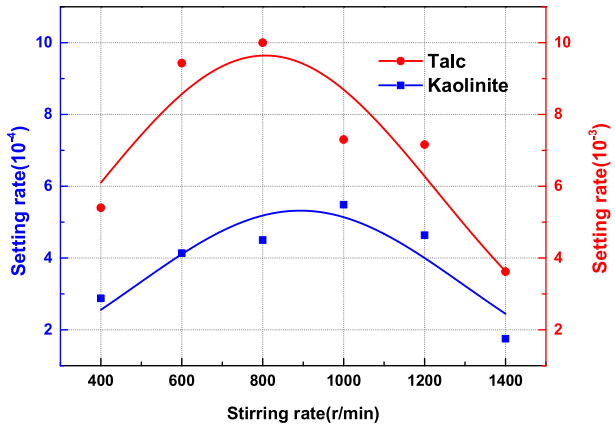

Fig. 11. Effect of stirring rate on setting rate.

highly symmetrical and nonpolar siloxane structure [50]. The results show that siloxane surface was very hydrophobic, while the hydroxyl surface was hydrophilic. Thus, based on the quite hydrophobic character of siloxane surface, a strong hydrophobic attraction between the siloxane surfaces may lead to a very powerful hydrophobic agglomeration behaviors of clay minerals in aqueous solution.

3.2. Effect of siloxane structure on the agglomeration degree

Effect of kerosene addition on aggregation degree was shown in Fig. 8. With the increase of kerosene addition, the aggregation degree of both talc and kaolinite increased originally, and then remained almost constant. The enhancement of aggregation degree by kerosene could be attributed to increase in particle adhesive strength caused by kerosene connect the siloxane [51]. Whereas, there were no obvious siloxane space presented in the agglomerates for kerosene, which resulted in the agglomeration degree reach a plateau. Under the same kerosene dosage, the agglomeration degree of talc was larger than that of kaolinite. Due to the much more exposed siloxane structure, much more talc particles are aggregated into larger flocs, which leads to the larger aggregation degree.

Mechanical agitation was necessary used for endowing the particles enough kinetics to overcome the potential energy barrier [52]. Effect of stirring rate on aggregation degree was shown in Fig. 9, as the increase of stirring rate, the aggregation degree of both talc fines and kaolinite fines increased. Because the kinetic energy input increased, the collision probability of particles was larger, therefore formed more flocs. And the agglomerate degree reached the equilibrium, resulting to the maximum aggregation behaviors. Under the same stirring rate, the agglomeration degree of talc was larger than that of kaolinite. It could be concluded that more siloxane on talc surfaces resulted in higher collision probability between talc particles and kerosene droplets. As a result, talc particles formed more flocs than kaolinite particles, which lead to the larger aggregation degree.

3.3. Effect of siloxane structure on the flocs sizes

According to Eqs. (1) and (2), turbidity on the basis of settling time had been fitted to certain functions. The setting rate K calculated in relation to Eq. (3) was used for evaluating the hydrophobic agglomeration performance. As the kerosene dosage increased, the setting rate of both talc and kaolinite first increased and then faintly decreased which was presented in Fig. 10. There was an optimized kerosene dosage to achieve the maximum setting rate. The emulsified nonpolar oil attached to the hydrophobic particles to reinforce the surface hydrophobicity, and then more particles agglomerated together to generate stronger and larger flocs [53,54]. The excessive dosage of kerosene lead to high viscosity which made the slightly decrease of setting rate of both

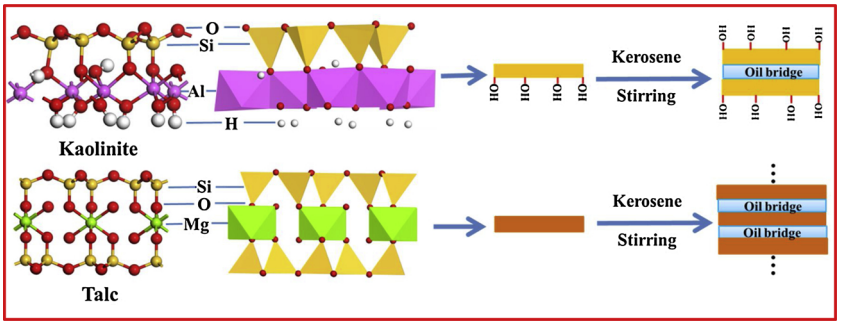

Fig. 12. The schematic diagram of agglomeration differences.

talc and kaolinite flocs [14,55]. Under the same kerosene addition, the setting rate of talc was one order of magnitude larger than that of kaolinite. Because the addition of kerosene adhered on the siloxane area could intensify the surface hydrophobicity. And the area of siloxane on talc was larger than that on kaolinite, which resulted in oil bridge connect the siloxane surface of talc layer by layer, and then formed stronger and larger flocs. Thus talc with two siloxane surfaces could be connected layer by layer, much larger flocs sizes formed than kaolinite with one siloxane surface.

The setting rate of both talc fines and kaolinite fines affected by stirring rate were exhibited in Fig. 11. As shown, both talc fines and kaolinite fines first increased and then declined with increase of the stirring speed. There was an optimized stirring speed to achieve the best hydrophobic agglomeration [3,56]. At low stirring rate, the collision probability of particles in suspension was small, resulting in irregular and loose agglomerates. Under high stirring rate, the agglomerates were broken up because of the very strong shear forces [57,58]. Both increasing and decreasing rate of setting rate of talc were larger than that of kaolinite, because talc with two siloxane surfaces was easily influenced by stirring rate. Under the same stirring rate, the setting rate of talc was one order of magnitude larger than that of kaolinite. Due to the area of siloxane on talc was larger than that on kaolinite, which resulted in higher collision probability between talc particles and kerosene than that between kaolinite particles and kerosene. Then oil bridge connected the siloxane surface of talc layer by layer, formed stronger and larger flocs than kaolinite.

3.4. Mechanism of siloxane affects hydrophobic agglomeration

Clay minerals surfaces dominated by siloxane were hydrophobic, which were demonstrated by MDs in this work. Kerosene addition provided the oil bridge to connected the siloxane surface of kaolinite, and then formed flocs. However, the another basal surface of kaolinite was full of hydroxyl groups, which was very hydrophilic and could not interact with kerosene molecules again. As a result, the kaolinite could only form very small flocs because oil can only spread on one kaolinite surfaces and interact with another oil spread kaolinite surface. On the contrary, talc is consisted of two basal siloxane surfaces, both can interact with the kerosene and then to bridge the other oil wetted talc. Hence, the probability of collision between talc with more area of siloxane surfaces and kerosene was higher than that between kaolinite, which lead to more flocs formed than kaolinite particles. Besides, talc consists of two siloxane surfaces, which resulted in oil bridge connect the siloxane surface of talc layer by layer, and then formed stronger and larger flocs than kaolinite, which were schematic shown in Fig. 12.

4. Conclusions

(1) Siloxane structure on clay mineral surface is of strong hydrophobicity, the number of which is correlated to the agglomeration degree and flocs size of clay minerals.
(2) Due to the much more exposed siloxane structures on talc surface, the hydrophobic agglomeration degrees of talc are far stronger than that of kaolinite.
(3) The sizes of talc flocs were also far larger than that of kaolinite due to both basal siloxane structures on talc surface and the formation of layer by layer floc structures.

Acknowledgements

The financial supports to this work from the National Natural Science Foundation of China under the projects No. 51674183 and 51874220 are gratefully acknowledged. This research is also supported by the financial supports for this work from Natural Science Foundation of Hubei Province of China (2018CFB468).

References

[1] L. Liang, Y. Peng, J. Tan, G. Xie, A review of the modern characterization techniques for flocs in mineral processing, Miner. Eng. 84 (2015) 130–144, https://doi.org/10.1016/j.mineng.2015.10.011.
[2] A. Mierczynska-Vasilev, M. Kor, J. Addai-Mensah, D.A. Beattie, The influence of polymer chemistry on adsorption and flocculation of talc suspensions, Chem. Eng. J. 220 (2013) 375–382, https://doi.org/10.1016/j.cej.2012.12.080.
[3] S. Lu, Y. Ding, J. Guo, Kinetics of fine particle aggregation in turbulence, Adv. Colloid Interface Sci. 78 (1998) 197–235, https://doi.org/10.1016/S0001-8686(98)00062-1.
[4] F. Rao, F.J. Ramirez-Acosta, R.J. Sanchez-Leija, S. Song, A. Lopez-Valdivieso, Stability of kaolinite dispersions in the presence of sodium and aluminum ions, Appl. Clay Sci. 51 (2011) 38–42, https://doi.org/10.1016/j.clay.2010.10.023.
[5] R. Guégan, E. Veron, L. Le Forestier, M. Ogawa, S. Cadars, Structure and dynamics of nonionic surfactant aggregates in layered materials, Langmuir 33 (2017) 9759–9771, https://doi.org/10.1021/acs.langmuir.7b01831.
[6] S. Sinha Ray, M. Okamoto, Polymer/layered silicate nanocomposites: a review from preparation to processing, Prog. Polym. Sci. 28 (2003) 1539–1641, https://doi.org/10.1016/j.progpolymsci.2003.08.002.
[7] S. Kang, Y. Zhao, W. Wang, T. Zhang, T. Chen, H. Yi, F. Rao, S. Song, Removal of methylene blue from water with montmorillonite nanosheets/chitosan hydrogels as adsorbent, Appl. Surf. Sci. 448 (2018) 203–211, https://doi.org/10.1016/j.apsusc.2018.04.037.
[8] S.S. Ray, M. Bousmina, Biodegradable polymers and their layered silicate nanocomposites: in greening the 21st century materials world, Prog. Mater. Sci. 50 (2005) 962–1079, https://doi.org/10.1016/j.pmatsci.2005.05.002.
[9] W. Wang, Y. Zhao, H. Yi, T. Chen, S. Kang, H. Li, S. Song, Preparation and characterization of self-assembly hydrogels with exfoliated montmorillonite nanosheets and chitosan, Nanotechnology 29 (2018), https://doi.org/10.1088/1361-6528/aa9ba4.
[10] J. Yao, H. Han, Y. Hou, E. Gong, W. Yin, A method of calculating the interaction energy between particles in minerals flotation, Math. Prob. Eng. 2016 (2016) 1–13, https://doi.org/10.1155/2016/8430745 Article ID 8430745.
[11] G. Lagaly, S. Ziesmer, Colloid chemistry of clay minerals: the coagulation of montmorillonite dispersions, Adv. Colloid Interface Sci. 100–102 (2003) 105–128, https://doi.org/10.1016/S0001-8686(02)00064-7.
[12] Y. Hu, L. Liu, F. Min, M. Zhang, S. Song, Hydrophobic agglomeration of colloidal kaolinite in aqueous suspensions with dodecylamine, Colloids Surf. A: Physicochem. Eng. Aspects 434 (2013) 281–286, https://doi.org/10.1016/j.colsurfa.2013.05.074.
[13] T. Chen, Y. Zhao, S. Song, Electrophoretic mobility study for heterocoagulation of montmorillonite with fluorite in aqueous solutions, Powder Technol. 309 (2017) 61–67, https://doi.org/10.1016/j.powtec.2016.12.086.
[14] B. Yang, S. Song, Hydrophobic agglomeration of mineral fines in aqueous suspensions and its application in flotation: a review, Surf. Rev. Lett. 21 (2014) 1430003, https://doi.org/10.1142/S0218625X14300032.

[15] S. Lu, Hydrophobic interaction in flocculation and flotation 3. Role of hydrophobic interaction in particle-bubble attachment, Colloids Surf. 57 (1991) 73–81, https://doi.org/10.1016/0166-6622(91)80181-M.
[16] I. Cengiz, E. Sabah, S. Ozgen, H. Akyildiz, Flocculation of fine particles in ceramic wastewater using new types of polymeric flocculants, Polym. Polym. Compos. 21 (2008) 449–456, https://doi.org/10.1002/app.29508.
[17] K. Das, S. Raha, P. Somasundaran, Effect of polyacrylic acid molecular weight on the floc stability during prolonged settling, Colloids Surf. A: Physicochem. Eng. Aspects 351 (2009) 1–8, https://doi.org/10.1016/j.colsurfa.2009.08.026.
[18] P. Ofori, A.V. Nguyen, B. Firth, C. McNally, M.A. Hampton, The role of surface interaction forces and mixing in enhanced dewatering of coal preparation tailings, Fuel 97 (2012) 262–268, https://doi.org/10.1016/j.fuel.2012.02.048.
[19] P. Watson, R. Farinato, T. Fenderson, M. Hurd, P. Macy, A. Mahmoudkhani, Novel polymeric additives to improve oil sands tailings consolidation, Proc. SPE Int. Symp. Oilf. Chem. 2 (2011) 703–709, https://doi.org/10.2118/141398-MS.
[20] Q.D. Nguyen, D.V. Boger, Application of rheology to solving tailings disposal problems, Int. J. Miner. Process. 54 (1998) 217–233, https://doi.org/10.1016/S0301-7516(98)00011-8.
[21] J.B. Farrow, R.R.M. Johnston, K. Simic, J.D. Swift, Consolidation and aggregate densification during gravity thickening, Chem. Eng. J. 80 (2000) 141–148, https://doi.org/10.1016/S1383-5866(00)00083-6.
[22] A. Sworska, J.S. Laskowski, G. Cymerman, Flocculation of the syncrude fine tailings part I. Effect of pH, polymer dosage and Mg2+ and Ca2+ cations, Int. J. Miner. Process. 60 (2000) 143–152, https://doi.org/10.1016/S0301-7516(00)00012-0.
[23] G. Gillies, K. Büscher, M. Preuss, M. Kappl, H.J. Butt, K. Graf, Contact angles and wetting behaviour of single micron-sized particles, J. Phys. Condens. Matter 17 (2005), https://doi.org/10.1088/0953-8984/17/9/011.
[24] H. Malandrini, F. Clauss, S. Partyka, J. Douillard, Interactions between talc particles and water and organic solvents, J. Colloid Interface Sci. 194 (1997) 183–193, https://doi.org/10.1006/jcis.1997.5103.
[25] T. Chen, Y. Zhao, S. Song, Comparison of colloidal stability of montmorillonite dispersion in aqueous NaCl solution with in alcohol-water mixture, Powder Technol. 322 (2017) 378–385, https://doi.org/10.1016/j.powtec.2017.09.032.
[26] Y.I. Tarasevich, E.V. Aksenenko, Interaction of water molecules with hydrophilic and hydrophobic surfaces of colloid particles, J. Water Chem. Technol. 37 (2015) 224–229, https://doi.org/10.3103/S1063455X15050033.
[27] W.F. Jaynes, S.A. Boyd, Hydrophobicity of siloxane surfaces in smectites as revealed by aromatic hydrocarbon adsorption from water, Clays Clay Miner. 39 (1991) 428–436, https://doi.org/10.1346/CCMN.1991.0390412.
[28] R. Šolc, M.H. Gerzabek, H. Lischka, D. Tunega, Wettability of kaolinite (001) surfaces - molecular dynamic study, Geoderma 169 (2011) 47–54, https://doi.org/10.1016/j.geoderma.2011.02.004.
[29] X. Yin, J.D. Miller, Wettability of kaolinite basal planes based on surface force measurements using atomic force microscopy, Miner. Metall. Process. 29 (2012) 8.
[30] L.S. Vienna, G.F. Haberhauer, L.S. Vienna, Solvation Effects on Molecules and Biomolecules, Springer, Netherlands, 2008, https://doi.org/10.1007/978-1-4020-8270-2.
[31] S. Song, A. Lopez-Valdivieso, Y. Ding, Effects of nonpolar oil on hydrophobic flocculation of hematite and rhodochrosite fines, Powder Technol. 101 (1999) 73–80, https://doi.org/10.1016/S0032-5910(98)00150-8.
[32] H. Yi, Y. Zhao, F. Rao, S. Song, Hydrophobic agglomeration of talc fines in aqueous suspensions, Colloids Surf. A: Physicochem. Eng. Aspects 538 (2018) 327–332, https://doi.org/10.1016/j.colsurfa.2017.11.017.
[33] S. Duzyol, A. Ozkan, Correlation of flocculation and agglomeration of dolomite with its wettability, Sep. Sci. Technol. 46 (2011) 876–881, https://doi.org/10.1080/01496395.2010.527895.
[34] C. Liu, G. Zhu, S. Song, H. Li, A novel method to improve carboxymethyl cellulose performance in the flotation of talc, Miner. Eng. 131 (2019) 23–27.
[35] K. van Netten, R. Moreno-Atanasio, K.P. Galvin, Selective agglomeration of fine coal using a water-in-oil emulsion, Chem. Eng. Res. Des. 110 (2016) 54–61, https://doi.org/10.1016/j.cherd.2016.02.029.
[36] Y. Hu, X. Liu, Z. Xu, Role of crystal structure in flotation separation of diaspore from kaolinite, pyrophyllite and illite, Miner. Eng. 16 (2003) 219–227, https://doi.org/10.1016/S0892-6875(02)00368-0.
[37] K.P. Galvin, K. van Netten, A new method for ultra-fast concentration of hydrophobic particles, Chem. Eng. Sci. 158 (2017) 439–444, https://doi.org/10.1016/j.ces.2016.10.049.
[38] H. Yi, X. Zhang, Y. Zhao, L. Liu, S. Song, Molecular dynamics simulations of hydration shell on montmorillonite (001) in water, Surf. Interface Anal. 48 (2016) 976–980, https://doi.org/10.1002/sia.6000.
[39] H. Li, Y. Zhao, S. Song, Y. Hu, Y. Nahmad, Delamination of Na-montmorillonite particles in aqueous solutions and isopropanol under shear forces, J. Dispers. Sci. Technol. 38 (2016) 1117–1123.
[40] B. Shi, V.K. Dhir, Molecular dynamics simulation of the contact angle of liquids on solid surfaces, J. Chem. Phys. 130 (2009) 34705, https://doi.org/10.1063/1.3055600.
[41] B. Ohler, W. Langel, Molecular dynamics simulations on the interface between Titanium Dioxide and water droplets: a new model for the contact angle, J. Phys. Chem. C 113 (2009) 10189–10197, https://doi.org/10.1021/jp811257x.
[42] H. Li, S. Song, X. Dong, F. Min, Y. Zhao, C. Peng, Y. Nahmad, Molecular dynamics study of crystalline swelling of montmorillonite as affected by interlayer cation hydration, JOM 70 (2018) 479–484, https://doi.org/10.1007/s11837-017-2666-2.
[43] H. Yi, F. Jia, Y. Zhao, W. Wang, S. Song, H. Li, C. Liu, Surface wettability of montmorillonite (0 0 1) surface as affected by surface charge and exchangeable cations: a molecular dynamic study, Appl. Surf. Sci. 459 (2018) 148–154, https://doi.org/10.1016/j.apsusc.2018.07.216.
[44] Y. Yuan, W. Zhan, H. Yi, Y. Zhao, S. Song, Molecular dynamics simulations study for the effect of cations hydration on the surface tension of the electrolyte solutions, Colloids Surf. A: Physicochem. Eng. Aspects 539 (2018) 80–84, https://doi.org/10.1016/j.colsurfa.2017.12.005.
[45] H. Yi, Y. Zhao, S. Song, Hydrophobic agglomeration kinetics of fine kaolinite particles in aqueous suspensions, J. Dispers. Sci. Technol. 38 (2017) 1336–1341, https://doi.org/10.1080/01932691.2016.1237366.
[46] D.L. Bish, Rietveld refinement of the kaolinite structure at 1.5 K, Clays Clay Miner. 41 (1993) 738–744, https://doi.org/10.1346/CCMN.1993.0410613.
[47] H. Du, J.D. Miller, A molecular dynamics simulation study of water structure and adsorption states at talc surfaces, Int. J. Miner. Process. 84 (2007) 172–184, https://doi.org/10.1016/j.minpro.2006.09.008.
[48] D. Tunega, L. Benco, G. Haberhauer, M.H. Gerzabek, H. Lischka, Ab initio molecular dynamics study of adsorption sites on the (001) surfaces of 1:1 dioctahedral clay minerals, J. Phys. Chem. B 106 (2002) 11515–11525, https://doi.org/10.1021/jp026391g.
[49] X.L. Hu, A. Michaelides, Water on the hydroxylated (0 0 1) surface of kaolinite: from monomer adsorption to a flat 2D wetting layer, Surf. Sci. 602 (2008) 960–974, https://doi.org/10.1016/j.susc.2007.12.032.
[50] M. Lundgren, N.L. Allan, T. Cosgrove, N. George, Wetting of water and water / ethanol droplets on a non-polar surface: a molecular dynamics study, Langmuir (2002) 10462–10466, https://doi.org/10.1021/la026191w.
[51] S. Song, S. Lu, Y. Zhang, A. Lopez-Valdivieso, T. Fort, Aggregation rate of fine particles in turbulent flows, J. Dispers. Sci. Technol. 25 (2004) 67–74, https://doi.org/10.1081/DIS-120027670.
[52] B. Yang, S. Song, A. Lopez-Valdivieso, Morphology of hydrophobic agglomerates of molybdenite fines in aqueous suspensions, Sep. Sci. Technol. 50 (2015) 1560–1564, https://doi.org/10.1080/01496395.2014.975365.
[53] A. Ozkan, Z. Uslu, S. Duzyol, H. Ucbeyiay, Correlation of shear flocculation of some salt-type minerals with their wettability parameter, Chem. Eng. Process. Process Intensif. 46 (2007) 1341–1348, https://doi.org/10.1016/j.cep.2006.10.018.
[54] S. Song, Hydrophobic Flocculation Applied to Fine Mineral and Coal Processing Mineral and Coal Processing Profesor Investigador, (1999).
[55] X.Q. Wu, A.J. Monhemius, R.J. Gochin, Quantitative assessment of hydrophobic agglomeration performance, Miner. Eng. 18 (2005) 567–573, https://doi.org/10.1016/j.mineng.2004.09.005.
[56] D.P. Patil, J.R.G. Andrews, P.H.T. Uhlherr, Shear flocculation-kinetics of floc coalescence and breakage, Int. J. Miner. Process. 61 (2001) 171–188, https://doi.org/10.1016/S0301-7516(00)00036-3.
[57] J. Ren, S. Song, A. Lopez-Valdivieso, J. Shen, S. Lu, Dispersion of silica fines in water-ethanol suspensions, J. Colloid Interface Sci. 238 (2001) 279–284, https://doi.org/10.1006/jcis.2001.7471.
[58] C. Liu, G. Zhu, S. Song, H. Li, Flotation separation of smithsonite from quartz using calcium lignosulphonate as a depressant and sodium oleate as a collector, Miner. Eng. 131 (2019) 385–391.